DEVICE CHARACTERISTICS OF VLWIR MCT PHOTODIODES

August 1999

R.E. DeWames, P.S. Wijewarnasuriya, W. McLevige, D. Edwall, G. Hildebrandt, and J.M. Arias
Rockwell Science Center, LLC, Thousand Oaks, CA 91360

A. D'Souza
Boeing Sensor Products

ABSTRACT

We have characterized the current-voltage characteristics, spectral response and quantum efficiencies of $Hg_{1-x}Cd_xTe$ photodiodes with x values equal to .209 and .194. The devices studied are double layer planar heterojunction (DLPHJ) photodiodes fabricated by MBE. Arsenic ion implantation is used to form the heavily doped p-side. The base is indium-doped at carrier density levels of ~ $5x10^{14}cm^{-3}$. For x = 0.194 at T = 30K, the bandgap wavelength, λ_g, is 22 μm. The reported IV's characteristics mostly deal with the behavior of small diodes, whereas the spectral response and quantum efficiencies are obtained from measurements on large diodes. Model calculations of the spectral response and quantum efficiencies are found to be in good agreement. For the device architecture with x = .209, a good fit to the zero-bias impedance area product R_0A is obtained using current expressions for diodes of small geometries. From this analysis, we obtained for the hole minority carrier mobility a value of 610 cm^2/v-sec at T = 78K. This result is considered to be an independent measurement of μ_h. For the case with x = .194, we observe significant deviation in the current-density-temperature characteristics from those expected from ideal diode model calculations. Specifically, the optical bandgap obtained from the spectral response is significantly different from the electrical bandgap obtained from the temperature dependence of dark currents. This is in contrast with prior reported work for material with x = .194, where good agreement was observed between measured and calculated characteristics. Some of the I-V features of the recent devices support that the p-n junction is situated in the graded region and this could account for some of the observed electrical behavior. For devices of excellent quality, we observe temperature-assisted tunneling current mechanisms at T = 5K, i.e., bumps in the relatively low forward bias region. This is a notable result considering that λ_g (5K) ≅ 25 μm, Eg. (5K) ≅ .05 eV.

1.0 INTRODUCTION

Sensors with capabilities to detect electromagnetic radiation in the wavelength region ≥ 14 μm are of interest for applications ranging from satellite remote sensing to surveillance. The standard detection materials for such applications are HgCdTe alloys with composition adjusted in the LWIR → VLWIR. For fundamental reasons, HgCdTe can have high responsivity and excellent noise performance at relatively high temperatures. However, these fundamental attributes are countered by difficulties in fabricating relatively large VLWIR detector, due to material and processing problems. To overcome these problems, it is important to conduct research in material science to identify the physical sources limiting performance, uniformity and yield. To reduce the deleterious electrical effects

Form SF298 Citation Data

Report Date *("DD MON YYYY")* 00081999	**Report Type** N/A	**Dates Covered (from... to)** *("DD MON YYYY")*

Title and Subtitle Device Characteristics of VLWIR MCT Photodiodes	**Contract or Grant Number**
	Program Element Number
Authors	**Project Number**
	Task Number
	Work Unit Number
Performing Organization Name(s) and Address(es) Rockwell Science Center, LLC Thousand Oaks, CA 91360	**Performing Organization Number(s)**
Sponsoring/Monitoring Agency Name(s) and Address(es)	**Monitoring Agency Acronym**
	Monitoring Agency Report Number(s)
Distribution/Availability Statement Approved for public release, distribution unlimited	
Supplementary Notes	
Abstract	
Subject Terms	
Document Classification unclassified	**Classification of SF298** unclassified
Classification of Abstract unclassified	**Limitation of Abstract** unlimited
Number of Pages 8	

caused by an inventory of localized defects; W.V. McLevige et al[1] developed the lateral collection diode architecture. For this structure, the electrical junction area is substantially smaller than the optical collection area. The ultimate approach to this technical product strategy to limit the effects of defects is to use a single small area diode in each pixel in conjunction with backside microlenses to focus the light within the collection area of the small diode.[2] Given this product strategy, it is important to understand the optoelectronic properties of devices of small geometries, since reduction of the size of the p-n junction increases the importance of the junction periphery.[3]

What follows is structured into three sections. Section 2 is a brief description of the spectral response characteristics for VLWIR photodiodes and measured values of the quantum efficiencies for devices of large geometries. The remarkable result of this data is the sharp rise in the spectral response, suggesting minimum bandgap tails in the characteristics of the absorption coefficient for VLWIR photodiodes.

Section 3 contains data and analysis of cases where the photodiode IV characteristics are found to be in good agreement with model calculations. Distinct features in trap assisted tunneling are observed suggesting distinct bandgap states close to mid-gap for material $E_g \cong .05$ ev at T = 5K. These distinct features are only observed in diodes of high quality. Also included is data and analysis for diodes of small geometries, $\lambda_g \cong 14$ μm at 40K, where good agreement is obtained between calculated and measured values. The hole minority carrier mobility, μ_h (T), was obtained by fitting the temperature dependence of the R_0A product for small diodes to a 2D analytical model.(3)

In section 4, we describe a case where the diode IV characteristics exhibit significant deviations from model calculations. The dominant deviation is observed in the temperature dependence of the current density and R_0A product. Essentially, different activation energies are obtained from the spectral response and the temperature dependence of the dark currents. Conclusions are contained in section 5.

2.0 SPECTRAL RESPONSE AND QUANTUM EFFICIENCY FOR VLWIR

Figure 1 illustrates the good agreement between the calculated spectral response and the experimental data. References to the parameters used in the model calculations are cited in the paper by G.M. Williams and R.E. DeWames [4]. Note the sharp onset of absorption and departure from the model in the absorption tail. This feature appears to be observed in VLWIR photodiodes and suggests that band tail states, if present, may not be optically active. The measured quantum efficiency at $\lambda = 9$ μm for large diodes is 70% and the calculated value is 74% using the device parameters listed in the figure insert. The x value is obtained from the spectral response fit. In the model calculations, the value of the minority carrier mobility for material with x = .194 was taken to be, $\mu_h = 1783$ cm^2/V-sec. The Auger minority carrier lifetime $\tau_h = 2x10^{-6}$sec and $L_h = 49$ μm. Taking the thickness of the n-region to be $W_n = 17.6$ μm and the measured QE value of 70% we obtain for L_h a value of 35 μm. This value is to compared to 49 μm which suggests that μ_h and/or τ_h are lower than assumed in the model simulation. The μ_h used in the model calculations are obtained by taking the experimental value of μ_e(4) and multiplying by the ratio of the effective masses, m_e/m_h. This assumption most likely leads to μ_h values which are too high based on prior work where we determined μ_h for x = .209 material.[5] What is needed are independent measurements of μ_h and τ_h.

---

[1] W.V. McLevige, D.D. Edwall, J.G, Pasko, J. Bajaj, L.O. Bubulac, J.T. Viola, W.E. Tennant, K. Vural, J. Ellsworth, H. Vydyanath, R. Purvis, S.E. Anderson, and R.A. Ramos, 1995 IRIS Specialty Group Infrared Detectors, ERIM (1995).
[2] W.V. McLevige, D.L. Lee, H.O. Sankur, R. Bailey, D.D. Edwall, D.E. cooper, G. Hildebrandt, J.T. Montroy, J.M. Arias, K. Vural, D.J. Chiaverini, D.E. Molyneux, M.M. Salcido, E. Dines, R.A. Ramos, 1999 IRIS, Specialty Group Infrared Detectors, ERIM (1999).
[3] R.J. Briggs, IEDM, pp 165-168, 1981.
[4] G.M. Williams and R.E. DeWames, Journal of Electronic Materials, Vol. 24, No. 9, 1995
[5] R.E. DeWames, W.V. McLevige, D. Edwall, P. Wijewarnasuriya, and D'Souza, Extended Abstract, MCT Workshop, 1998

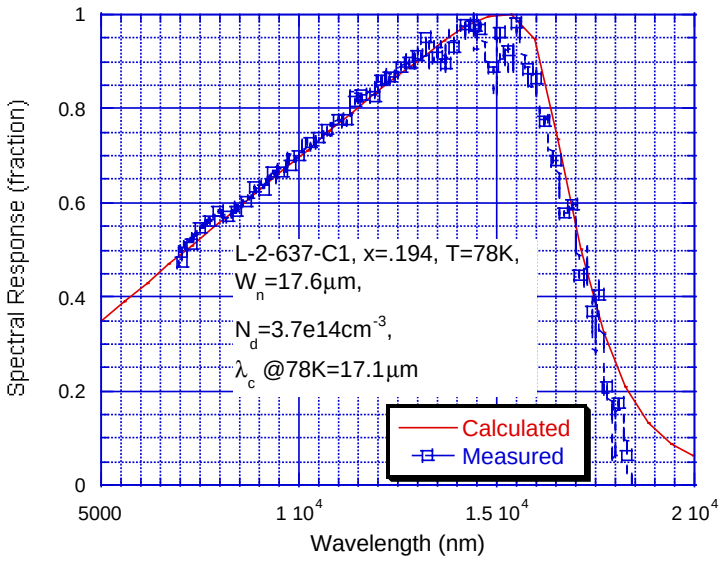

Figure 1. Measured vs calculated spectral response per Watt of VLWIR photodiodes.

3.0 EXAMPLE OF VLWIR PHOTODIODES CHARACTERISTICS EXHIBITING IDEAL DIODE CHARACTERISTICS

LWIR and VLWIR photovoltaic devices are dominated by dark currents of diffusion and tunneling origins. In our experience, no regions in the temperature and voltage dependence of the dark currents for LWIR and VLWIR is observed, suggesting thermal generations-recombination currents are not limiting the dark currents.[6] In addition, in general the tunneling currents are of the Zener type and defect dominated in contrast to band-to-band tunneling as expected from the ideal defect free diode current equations.

Figures 2 and 3 respectively, illustrate the R_0A product and dark currents versus temperature for a diode of λ_g = 22 µm at T = 30K. As reported in reference (4), the data can be fitted with diode equations for the defect free semiconductors. Parameters used in the fit are $N_d = 2x10^{15}cm^{-3}$, diode thickness equals 11 µm, junction depth = 1 µm, x = .194. The current equation for tunneling currents dependent on the shape of the potential barrier.[7] This feature changes the constant value in the exponential term from a value of 1 for the parabolic to 1.8 for the triangular potential.(6) To fit the experimental data a value of 1.4 was used. The example is notable because it does illustrate that MCT photodiodes at VLWIR are not fundamentally limited. Questions on the possibility of insurmountable barriers to build consistently high performance, reliable VLWIR focal plane arrays, due to technology limitations, remain to be answered.

---

[6] R.E. DeWames, J.G. Pasko, E.S. Yao, A.H.B. Vanderwyck and G.M. Williams, *J. Vac. Sci. Tech.* Ab (4), Jul.Aug 1988.
[7] J.L. Moll, Physics of Semiconductors (New York: McGraw Hill Book Co., 1964) p 253.

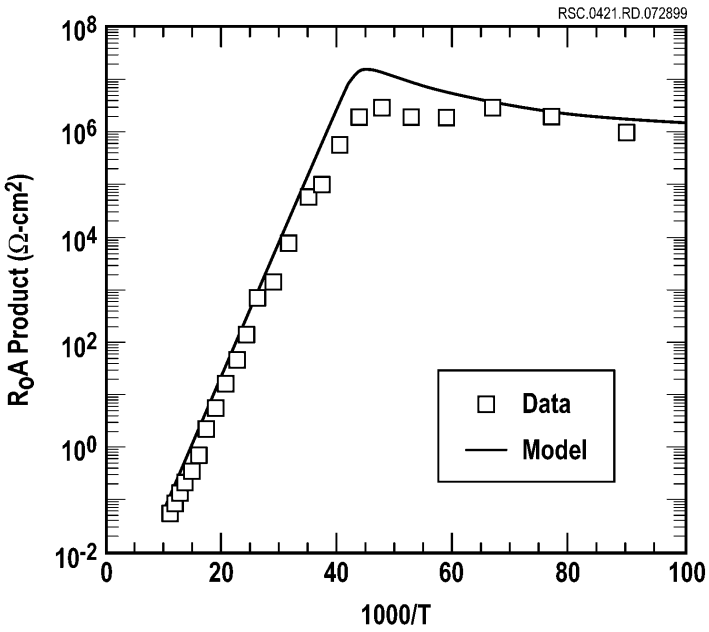

Figure 2. Calculated and measured R_0A products as a function of temperature.

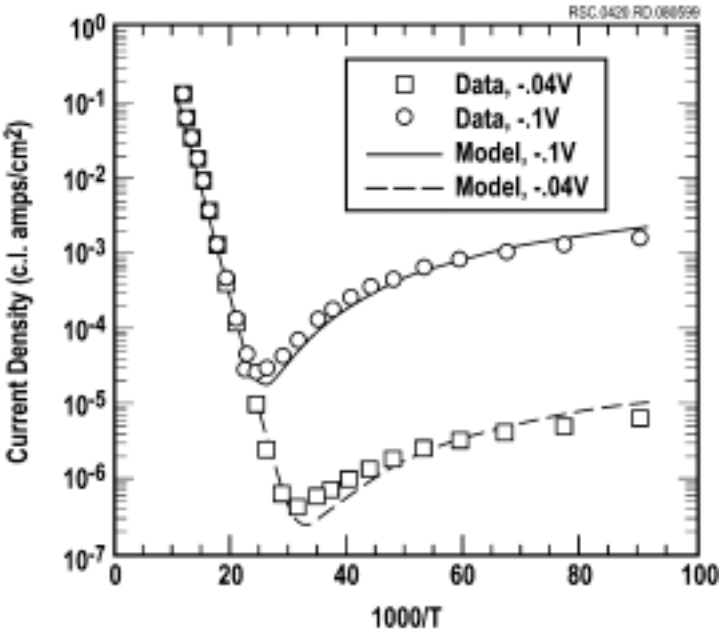

Figure 3. Calculated and measured current density vs. inverse temperature at two different reverse bias voltages for the detector from Fig. 2.

We proposed that the current mechanisms are diffusion limited and band-to-band tunneling as the basis of the fit to experimental data. Figure 4 illustrates the shape of the IV and dynamic resistance area product, R_dA, at T = 28K. In the small bias and forward bias region the R_dA data shows some deviations from an exponential current and this behavior becomes evident as illustrated in Fig. 5 for T = 5K. The bandgap is ~ .05 eV and we note that below this voltage value the behavior shows structure at about V = .03 volts. We propose that this behavior is caused by

trap assisted tunneling. In the very small forward and reverse bias region, the trend and analysis suggests band-to-band processes. This data on the IV characteristics at low temperature suggest the presence of bandgap states near mid-gap for VLWIR photodiodes. These features are not dominant in diodes of high quality, in the temperature region ≥ 30K, where according to the data in Figures 2 and 3, the dominant current is the small bias region is diffusion limited.

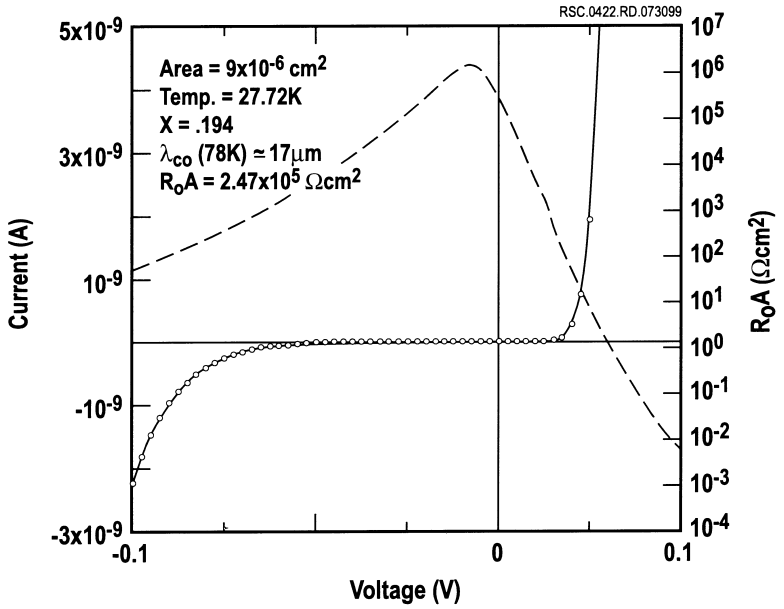

Figure 4. Measured current and dynamic resistance area product, R_dA vs. Voltage at T = 28K for the detector of Fig.2.

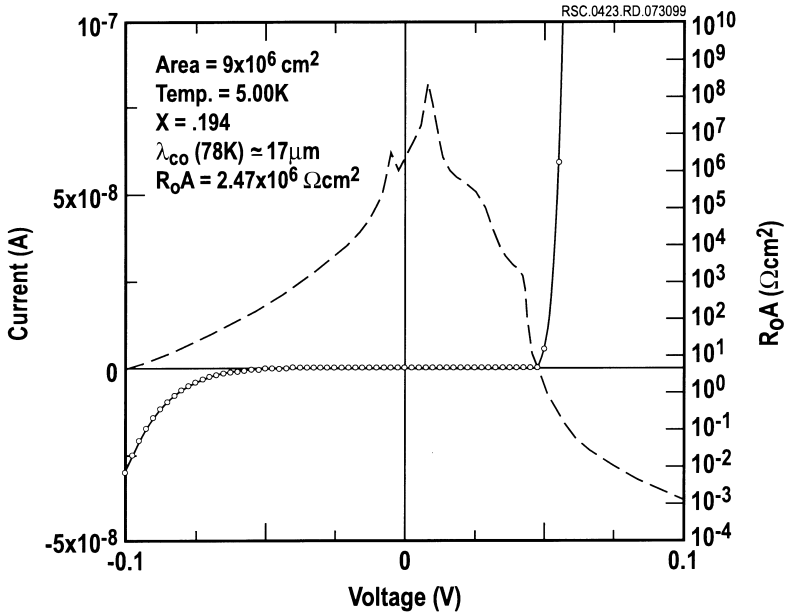

Figure 5. Measured current and dynamic resistance area product, R_dA vs. Voltage at T = 5K for the detector of Fig 2.

The data shown in Fig. 6 is an example of a case of where the diodes are of small size and under these conditions 3D models are needed to account for the effects of the periphery. The expression for the R_0A_j inserted in Fig. 6 was derived by Briggs, assuming the diode has spherical geometry. Brigg's showed that this approximation yields good agreement with his numerical simulation for long diodes of cylindrical geometry. We noted that this expression also represented his numerical results for short diodes, see Fig. 3, for the case $a/L_h < .3$, where a = radius of the diode and L_h = diffusion length, and $d_n/L_h \geq .5$, where d_n is the thickness of the n-type base of the diode. This expression suggests that for small diodes, the R_0A_j product depends on the minority carrier concentration, p_{no}, as expected, and the minority carrier mobility, μ_h. This is in contrast to the large diode case where for the short diode the dependence is on the minority carrier lifetime, τ_h. We noted that this result suggests that from diodes of large geometries one could obtain τ_h, and from small geometries μ_h. Such measurements provide the opportunity for self-consistent determination of the material parameters, since they enter such expressions as the quantum efficiency via the diffusion length, L_h. A value of 610 cm^2/v-sec at T = 78K for μ_h was determined from the R_0A_j fit. The majority carrier mobility, μ_e was independently measured on the active layer prior to device fabrication and agrees with the value used in the MCT library [4]. Also, the value of μ_h is in good agreement with the measured values reported in ref. 7, μ_h = 570 vm2/v-sec for material of nominal composition of x = .215.

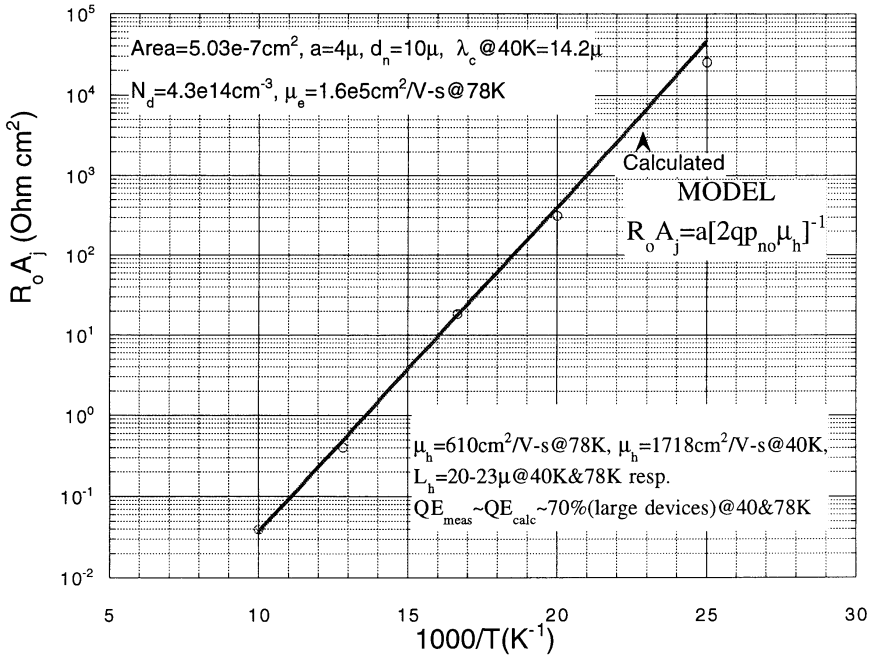

Figure 6. Measured and calculated small diode R_0A_j dependence on temperature.

4.0 EXAMPLE OF DARK CURRENT AND R_0A_j BEHAVIOR THAT DEVIATES FROM THE IDEAL DEFECT FREE DIODE MODEL.

Figure 7 is a plot of the current density for VLWIR photodiodes with x = .194, λ_{co} (30K) ≅ 23 μm. The carrier concentration is Nd = 3.7 x $10^{14}cm^{-3}$ for the n-side and ~ $10^{17}cm^{-3}$ for the p-side. At temperature > 75K, the n-side is essentially intrinsic and the model calculation is questionable. Diode behavior is observed as expected, since the p-side is heavily doped. It is interesting to note that the use of the simple model seems to account for the experimental data at high temperature. We have used the spherical model approximation for the current density and the values of μ_h were obtained by equating $\mu_h = \mu_e(m_e/m_h)$. This assumes the relaxation times are equal for both majority and minority carriers. This is likely not a valid assumption, based on our findings reported in section 3, where this

approximation would have yielded $m_e/m_h \cong 67$ at 78K in contrast to 262 obtained from the R_0A_j fit and independent measurements of μ_h.[8] For the purpose at hand what we take for μ_h is not critical, since our major message is the deviation between calculated and measured temperature dependence of the current density in the diffusion limited regime. This data suggests an effective activation energy, electrical bandgap, significantly different from the optical bandgap obtained by fitting the spectral response data for the large diodes, see Fig. 1. The increasing current density at low temperatures for increasing reverse bias voltage is due to tunneling mechanisms. The tunneling currents are of defect origin and not band-to-band, as described previously.

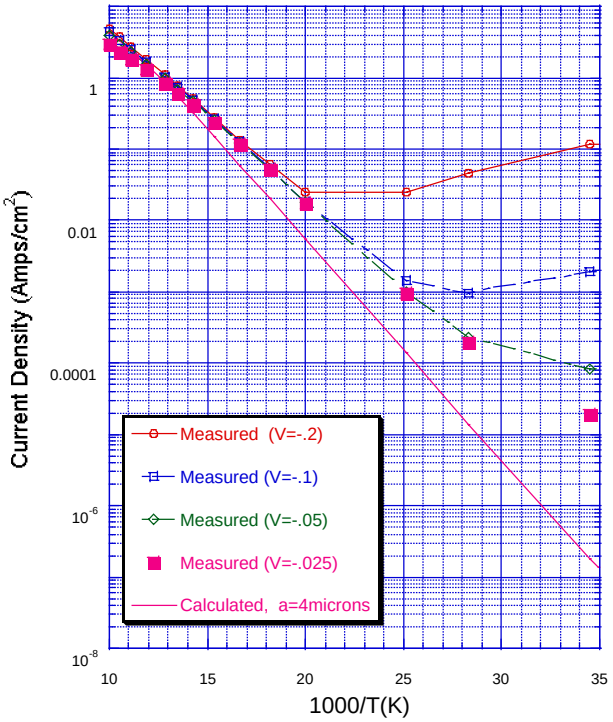

Figure 7. Current density as a function of temperature for VLWIR photodiodes.

Figure 8 illustrates the current density and R_0A_j as a function of temperature. A key observation is that for large reverse bias the experimental values for the current density are in better agreement with the simple model calculations. The bias dependence of the experimental values for the current density suggests that the p-n junction is situated in the graded region. The 2D model calculation for R_0A_j assumed that the voltage dependence of the current is qV/kt. In the intrinsic regime, the dependence is qV/2kt.[9] Therefore, the calculated values of R_0A_j ~ 100K should be multiplied by 2, in closer agreement with the experimental data. Figures 9 and 10, taken from reference 4, illustrate the effects of placing the p/n junction relative to the heterojunction. Figure 9 illustrates that lower dark current density should be expected in the small bias region if the p/n junction is moved into the larger bandgap material. Dark currents and photocurrents are proportionally affected as illustrated in Fig. 10. At this stage, we do not have a quantitative explanation for the deviations between measured and calculated values in the diffusion region of operation, T > 40K. The model we used to compare with the experimental data is a zero-order approximation to the 2D DLHJ structure. The fact that cases can be found where agreement is good is in fact remarkable.

---

[8] Y. Schacham-Diamand and I. Kidon, *J. Apl. Phys*, 15 August 1984.

[9] J. Lindmayer and C.Y. Wrigley, "Fundamentals of Semiconductor Devices," Van Nostrand Reinhold Company, 1965.

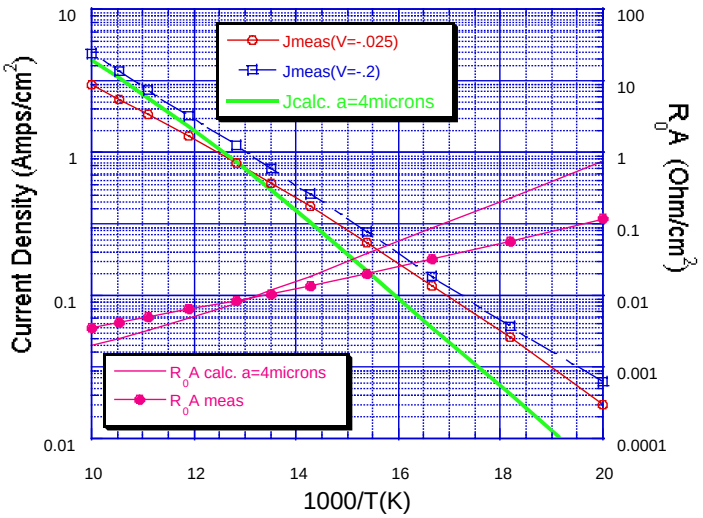

Figure 8. Current density and R_0A as a function of temperature for VLWIR small photodiodes.

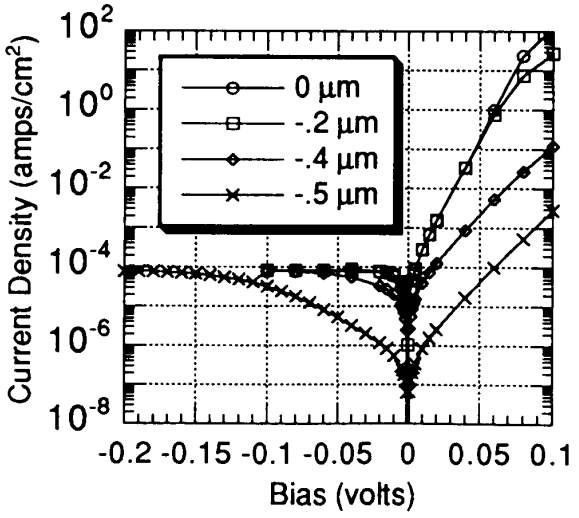

Figure 9. Calculated IV characteristics for a hetero-junction diode as a function of the placement of the p/n junction relative to the heterojunction.

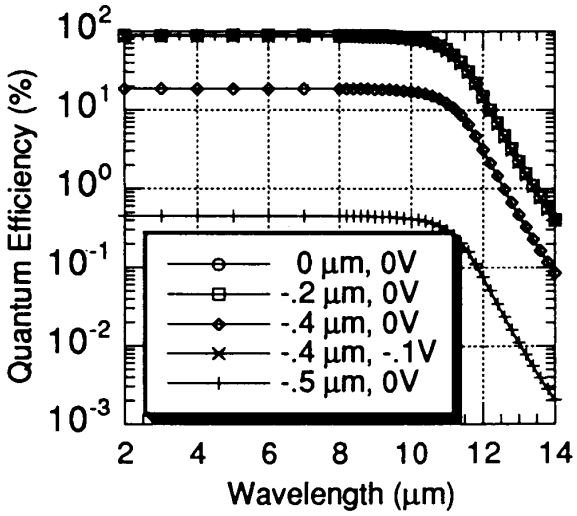

Figure 10. Calculated quantum efficiency for a hetero-junction diode as a function of the placement of the p/n junction relative to the heterojunction.

5.0 CONCLUSION

We discussed examples of diode behavior, which exhibit properties, which could be explained by defect free model simulations. We also discussed that situations occur that significant differences are observed even in the small diode behaviors, which purports to be defect free regions. We conjectured that the positions of the p/n junction and the quality of the interface material could be a cause for such departures from homojunction properties. The small diode geometry is expected to be more sensitive to this semiconductor interface, since the ion implantation profile is likely to be tear-drop-like. The cases reported are for different layers; two of the examples had an x value of .194. The anomalous behavior discussed in section 4 needs to be studied further, since small diodes are the basis for the lateral and microlens technology strategies to overcome the deleterious effects of localized defects. It is notable that diodes can be made at these VLWIR that obey simple defect free model simulations.